Slit Devolatilization of Polymers

Pier Luca Maffettone and Gianni Astarita
Dept. of Chemical Engineering, University of Naples, Italy

Laura Cori and Lino Carnelli
Enimont Anic Research Center, Bollate (MI), Italy

Franco Balestri
Montedipe Research Center, Mantova, Italy

A model of the process of polymer devolatilization in a heated slit is presented. Momentum, heat, and mass transfer in the slit are taken into consideration, and only one adjustable parameter is used. The model predicts pressure and temperature profiles, and residual volatile contents at the exit which are in good agreement with those measured in a single instrumented slit.

Introduction

A new static devolatilization technique, which overcomes the problem of long residence times of the polymer at high temperatures, has recently been developed (EP, 1990). The polymer solution is fed through an assembly of slits of rectangular cross section; the walls of the slits are kept at a high temperature by circulation of hot oil through holes in the slit walls. The slits feed into a flash chamber where vacuum is maintained.

While in the actual process an assembly of a very large number of slits is used, we have performed experiments on an instrumented single slit. In this paper, we present a mathematical model of the single-slit configuration. The model contains only one adjustable parameter; it predicts profiles of temperature, pressure, and residual volatile concentration that compare well with the measured results. Figure 1 is a sketch of the single-slit configuration.

A previous model (Maffettone and Astarita, 1990) entirely avoided the issue of the momentum balance in the polymeric phase by assuming that the pressure gradient was constant along the flow direction, and using the measured pressure drop as input data. While that model was reasonably successful in predicting temperature and concentration profiles, it was of course intrinsically unable to predict the pressure drop and the pressure profile.

The eventual aim of this research project is to develop a complete model capable not only of predicting the behavior of a given system, but one that can confidently be used for design of new processes. In this work, we have limited attention to the fundamental physical ideas on which the model is based, and in order to test their soundness without embarking on a major numerical effort, we have consistently made rather crude approximations whenever those were thought to induce at most an error of say 10%. Hence we only expect our model, at best, to predict the actual results to within such an error; should some of the fundamental physical ideas be wrong, much larger discrepancies would be expected. Since the model contains only one adjustable parameter, the test of comparison with experimental data is a severe one.

Physical Model

In the model presented by Maffettone and Astarita (1990), it was assumed that two layers of gas formed near the heated walls, the thickness of which was such as to give the required pressure drop due to viscous dissipation in the gas phase. However, should two gas layers indeed form, they would act

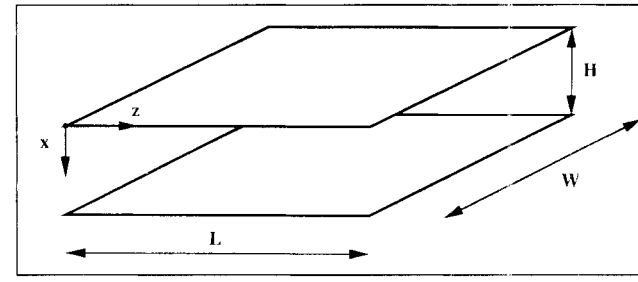

Figure 1. Single slit flow configuration.

Correspondence concerning this paper should be addressed to Gianni Astarita.

as lubricants for the polymer phase, and the momentum balance in the polymer could not be satisfied except for a physically unrealistic condition, as discussed in more detail below.

Since the volumetric gas flow rate is several orders of magnitude larger than that of the polymer over most of the slit, gas flow cannot be thought of as taking place in the form of gas bubbles in the polymer phase, and hence a continuous gas region leading to the exit must develop in the slit. There are many possible flow configurations one could imagine, but we restrict attention to only the following two. The first flow configuration is an asymmetric one, where a gas layer forms near one of the walls, with the polymer phase touching the other wall. This is a realistic possibility, but it does lead to a difficulty: the polymer phase becomes hotter on the side that touches the heated wall, and hence gas tends to form there, rather than on the side where there is a continuous gas phase. This probably means that, should this be the true flow configuration, the polymer would tend to switch from touching one wall to touching the other wall, giving rise to a cyclic behavior. Since cyclic behavior has in fact been observed experimentally, this difficulty could in fact explain it, although we do not claim that this is indeed the reason for the observed behavior. We develop a steady state model, in the belief that it should adequately describe the average values of variables, and thus we use for comparison the experimentally measured averages.

The other flow configuration we consider is a symmetric one, with the gas layer in the middle of the slit and two polymer layers forming near the walls. As will be seen, measured pressure drops are predicted better by using the equations that emerge from such a flow configuration; however, we do not claim this to prove that indeed the symmetric flow configuration is the correct one, since alternate explanations for the poorer fit obtained from the asymmetric flow configuration equations are possible. A minor conceptual difficulty with the symmetric flow configuration is that it is unstable to gravity. The single-slit experiments were conducted with a vertical slit, and hence this difficulty does not arise in this case.

Let $p^o(T, c)$ be the vapor pressure of the volatile component at temperature T and volatile mass fraction c. At the entrance of the slit, $c = c_o$, and $p^o(T_o, c_o)$ is guaranteed to be less than the local pressure p, otherwise flashing would start to occur before the solution enters the slit. It follows that there is an initial region of the slit where no devolatilization occurs. We will refer to this region as the heating section, and to the remaining part of the slit as the main section. In actual operation, the heating section constitutes only a small fraction of the entire slit, since most of it needs to be reserved for devolatilization to take place.

Let $Q(z)$ be the mass flow rate per unit slit width of the polymer phase at a distance z from the entrance to the slit, and let $Q_o = Q(0)$ be the feed flow rate per unit width. The wall is kept at some constant temperature T_w, while the feed is at temperature T_o, with $\omega = T_w - T_o$ the imposed driving force. We neglect non-Newtonian effects; let $\mu_P(z)$ be the viscosity of the polymer solution at the temperature and volatile concentration prevailing at position z. Since temperature varies by a significant amount along the slit, and the volatile mass fraction decreases from inlet values of the order of 0.5 to some 100 ppm at the exit, μ_P may change by several orders of magnitude along the slit.

The process we are considering is really made up of three interacting phenomena: momentum transfer, heat transfer, and mass transfer. We try to discuss these three aspects separately in the following, although, as will be seen, coupling between the three aspects is significant.

Momentum transfer

The polymer touches both walls in the heating section. As discussed in more detail below, we approximate the slit as two infinite parallel plates located a distance H apart. Thus, with ρ_P the polymer density, the momentum balance in the heating section is:

$$-\frac{dp}{dz} = \frac{12\mu_P Q}{\rho_P H^3} \tag{1}$$

The fluid mechanics in the main section in the slit geometry we are considering is a two-phase flow problem that is in principle a fully three-dimensional problem. A rather complete analysis of stratified creeping flow in a duct of rectangular cross section is given by Navratil DiAndreth (1984); ducts of arbitrary cross section have been considered by Yu and Sparrow (1967). Charles and Redberger (1967) considered a circular tube, and Charles and Lillehet (1967) a rectangular tube, for the case where the viscosities of the two fluids are widely different. A very considerable simplification arises if one is willing to approximate a rectangular cross section with an infinite slit geometry; this case is discussed by Bird et al. (1960). All of these works consider horizontal ducts, with the flow stably stratified against gravity, and they are restricted to the case of steady flow, so that nothing changes along the flow direction.

In our problem, the flow is certainly not steady, since the gas flow rate grows from zero at the entrance to significant values at the exit, the liquid phase viscosity changes by several orders of magnitude, and so on. We therefore make two important simplifications, which seem to be amply justified. First, we do approximate the rectangular cross section with an infinite slit, so that there are only two coordinates to take into account: the distance z from the entrance to the slit, and the distance x from one of the walls. Second, we use the lubrication approximation (Batchelor, 1967): the flow at any position z is the same one would have in steady state flow with the local values of flow rates and physicochemical parameters. Finally, although temperature is expected to depend on both z and x, we will assume that it changes little enough along x so that both phases can be regarded as having a viscosity that is independent of x. With these approximations, we essentially reduce the two-dimensional problem to two uncoupled one-dimensional problems.

Use of the lubrication approximation in the gas phase should be justified. The Reynolds number based on the gas layer thickness is G/μ_G, and therefore its highest value is at the exit, where it is still significantly less than 1,000, and the value of $d\delta/dz$ is invariably quite small, so that the classical conditions for the lubrication approximation are satisfied. The Reynolds number based on the eulerian inertia force (the axial acceleration of the gas) is significantly smaller, since with the same velocity scale the relevant length scale is the slit length rather than the gas layer thickness; however, it is unclear what the

upper limit for the latter Reynolds number is for the lubrication approximation to be valid, and some conceptual doubt exists here.

It is important to realize that the liquid phase in the main section may well contain significant amounts of gas bubbles: there is certainly a driving force for bubble formation, since $p^o > p$, and gas bubbles have been observed visually in the polymer phase exiting from the slit. As far as momentum transfer is concerned, gas bubbles of course have two effects: first, their presence increases the volumetric flow rate of the liquid phase, and second, the equivalent viscosity of the bubble-containing liquid is different from that of the suspending liquid. These difficulties are discussed in Appendix A; here we simply neglect this effect entirely. In this regard, there is an important point to be stressed. Since the total volumetric flow rate of the gas phase near the exit of the slit may be as much as 10^5 times the volumetric flow rate of polymer, any gas present in the form of gas bubbles constitutes an absolutely negligible fraction of the total, and hence from the viewpoint of mass balance the presence of the bubbles can certainly be neglected.

Let $\partial p/\partial z = -J$ be the local value of the axial pressure gradient, and let $\tau(x)$ be the local shear stress transverse distribution. The momentum balance in the z direction, without any constitutive assumptions about the fluid(s) in the channel, is:

$$\frac{\partial \tau}{\partial x} = -J \tag{2}$$

It follows that the shear stress distribution in the transverse direction is linear in every possible case. Now the first thought could be that it is symmetric as well, as implicitly assumed by Maffettone and Astarita (1990). In this case, τ would be 0 at the midplane $x = H/2$. This however would imply that the velocity gradient $\partial v/\partial x$ is zero at the midplane, and hence, unescapably, that the phase flowing in the middle has the largest velocity, while the phase flowing near the two walls moves more slowly. Now if the wall phase is the gas, one would conclude that the polymer velocity is the larger one, and since the gas phase volumetric flow rate may well be several orders of magnitude larger than the polymer phase flow rate, this would require the polymer phase to be thin to an absolutely unrealistic level. (If two gas layers form to encapsulate the more viscous polymeric phase, there can be no maximum of the gas velocity other than at the polymer interface, since Eq. 2 dictates that the shear stress cannot go to zero at some location in both gas layers.) This leaves only the two possibilities we consider: either an asymmetric distribution with the gas flowing near one wall, or a symmetric distribution with the gas phase flowing near the middle. Of course, flow configurations that are not constant along the slit width could be considered, but this would entail analysis of a fully three-dimensional problem.

We first consider the asymmetric case where the gas phase forms near one of the walls and the polymer touches the other wall. Let τ_o be the shear stress at the gas-phase wall (so that $\tau = \tau_o - Jx$), h the local thickness of the gas layer, and μ_G the gas viscosity. The velocity distribution in the gas phase is:

$$v = -\frac{Jx^2}{2\mu_G} + \frac{\tau_o}{\mu_G} x \tag{3}$$

Now let U be the velocity of the gas-polymer interface, which is located at $x = h$. One obtains:

$$\frac{\tau_o}{\mu_G} = \frac{U}{h} + \frac{Jh}{2\mu_G} \tag{4}$$

Let G and ρ_G be the mass flow rate of gas per unit slit width, and the gas density, respectively. Integrating Eq. 3 between 0 and h one obtains:

$$G = \rho_G \left(\frac{Uh}{2} + \frac{Jh^3}{12\mu_G} \right) \tag{5}$$

Now let $\epsilon = \mu_G/\mu_P$, which is guaranteed to be a very small number (ranging between 10^{-6} and 10^{-10} in the actual experimental conditions). In the polymer phase, which is located at $h \le x \le H$, the momentum balance yields, when terms of order ϵ are neglected with respect to terms of order unity:

$$v = U - \frac{J}{2\mu_P}(x^2 - hx) \tag{6}$$

With $\delta = h/H$, the no-slip condition at the $y = H$ wall yields the value of U—which, incidentally, is the order of magnitude of the polymer phase velocity:

$$U = \frac{JH^2}{2\mu_P}(1 - \delta) \tag{7}$$

Integration of Eq. 6 between h and H yields, after substitution of Eq. 7 and rearrangement, the polymer flow rate per unit slit width Q:

$$Q = \frac{\rho_P J H^3}{3\mu_P}\left(1 - \frac{9}{4}\delta + \frac{3}{2}\delta^2 - \frac{1}{4}\delta^3\right) \tag{8}$$

The velocity and shear stress distributions are shown in Figure 2. Notice that once the values of Q and G are assigned, Eqs. 5, 7, and 8 yield the values of U, J, and δ, and hence the problem is well posed.

The equations above can be considerably simplified. If Eq. 7 is substituted into Eq. 5, one realizes that with common terms canceled out, the two terms on the righthand side are of relative order of magnitude ϵ and δ^2. As will be seen, ϵ is

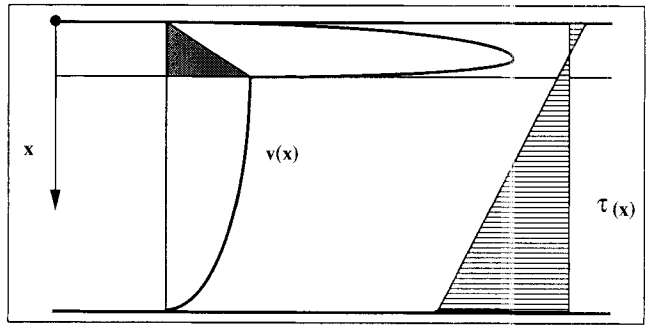

Figure 2. Velocity and stress transverse distributions for asymmetric flow configuration.

significantly less than δ^2, and hence the first term may be neglected in an order of magnitude analysis—this corresponds to neglecting the small shaded triangular area in Figure 2—yielding the following estimate of the order of magnitude of the gas flow rate:

$$G \approx \frac{\rho_G J h^3}{12\mu_G} \tag{9}$$

Since the term within parentheses in Eq. 8 is of order unity, the polymer flow rate estimate is:

$$Q \approx \frac{\rho_P J H^3}{3\mu_P} \tag{10}$$

Combination of these results yields:

$$\delta^3 \approx \frac{\epsilon \rho_P G}{4 Q \rho_G} \tag{11}$$

At the exit of the slit, ρ_P/ρ_G may be as large as 10^5, G/Q is of order unity (since the typical feed conditions are with a weight fraction of volatile of 0.5), and ϵ is of order 10^{-9}, yielding an estimate for δ of the order of 0.05. Near the beginning of the main section, ϵ may be as large as 10^{-6}, but ρ_P/ρ_G is only 10^3 and G/Q is significantly less than unity, so that one obtains the same estimate for δ. One may thus conclude that $\epsilon \ll \delta^2$, coherently with the initial assumption, and that $\delta \ll 1$.

Based on these considerations, we have further simplified the equations by neglecting terms of order δ. It would be comparatively easy to retain those terms in the numerical procedure, but we feel that the uncertainty concerning the actual values of polymer viscosity and volatile vapor pressure are large enough that an approximation of order δ is more than justified. Hence the momentum balances in the main section for the gas and polymer phase, respectively, are written as follows:

$$-\frac{\partial p}{\partial z} = \frac{3\mu_P Q}{\rho_P H^3} \tag{12}$$

$$-\frac{\partial p}{\partial z} = \frac{12\mu_G G}{\rho_G h^3} \tag{13}$$

The gas density needed in Eq. 13 is calculated from the ideal gas law by assuming that the gas temperature coincides with the wall temperature; since absolute temperatures are involved, this is a very good approximation to the actual gas density.

The second possible flow configuration (two polymer layers forming along the two walls) is examined along analogous lines; the final result is simply that the coefficient 3 in Eq. 12 becomes 12. The reason for this is that each polymer layer carries only half the flow rate (which by itself would make the coefficient half as big), but the available thickness, which enters the equation through its cube, is also one-half the previous one, thus increasing the coefficient by a factor of 8. The result can be rationalized also from a different viewpoint. In the symmetric configuration, the gas layer acts as a lubricant, reducing the velocity gradient near one of the walls from whatever it would be in the absence of a gas layer to essentially zero; in the symmetric configuration, the gas layer forms at the position where the velocity gradient would be zero anyhow, and hence it does not act as a lubricant. These considerations guarantee that the two flow configurations we consider are indeed the extreme ones, and that any other flow configuration would result in a coefficient between 3 and 12: when the gas layer forms at one of the walls, it has the highest possible lubricating effect; when it forms at the midplane, it has no lubricating effect whatsoever.

The analysis above is based on the lubrication approximation, and quantities appearing in it are in fact functions of z. The total and polymer mass balances between the entrance and a generic section furnish two relationships between $Q(z)$, $G(z)$, and $c(z)$:

$$Q_o = Q + G \tag{14}$$

$$Q_o(1 - c_o) = Q(1 - c) \tag{15}$$

Heat transfer

For both flow configurations, heat transfer occurs by conduction: coherently with our fluid mechanics modeling, the velocity vector is always pointing in the z direction, and hence there is no convective heat transfer in the transverse direction. We wish to write a heat balance in the polymer phase, and we need to express the local rate of heat supply from the walls. Let k_P be the polymer phase thermal conductivity, which will be regarded as a constant. (The presence of gas bubbles may in actual fact decrease the conductivity; this is discussed later.) T is the local mixing cup polymer temperature, Φ the local heat transfer coefficient, and $N = \Phi H/k_P$ the local Nusselt number at the polymer wall. In the heating section where there are two polymer walls, the heat flux is:

$$q = \frac{2k_P N(T_W - T)}{H} \tag{16}$$

This equation hold true also in the main section in the symmetric flow configuration.

The situation is more complex in the asymmetric flow configuration. Let T_I be the interface temperature, and $k_G = Kk_P$ be the gas-phase thermal conductivity, which is also assumed to be constant. The conductivity ratio K is typically of the order of 0.01. The heat flux through the gas phase is:

$$q_G = \frac{k_G(T_W - T_I)}{h} \tag{17}$$

However, the interface temperature is not known in advance. Let m be the Nusselt number in the polymer phase at the gas–polymer interface. Since q_G is also the heat flux into the polymer phase at the interface, one has (again to within order δ):

$$q_G = \frac{k_P m(T_I - T)}{H} \tag{18}$$

The interface temperature can be eliminated between Eqs. 17 and 18 to yield:

$$q_G = \frac{k_P}{H}\frac{1}{1/m + \delta/K}(T_W - T) \tag{19}$$

Since there is also a polymer wall, the heat flux in the main section is calculated as:

$$q = \frac{k_P}{H}\left(N + \frac{1}{1/m + \delta/K}\right)(T_W - T) \tag{20}$$

The real difficulty lies in the estimation of the Nusselt numbers N and m. In the heating section N is determined by the classical Graetz problem analysis (Drew, 1931; Jacob, 1949). The Graetz number for our case is of the order of 10, and hence well in the region where N is independent of it; the value from the classical analysis is 3.8. Physically, the reason for this is easy to understand: since the heating section is only a fraction of the total slit length, the slit is "long" in the Graetz problem sense, and hence the heat transfer coefficient has its asymptotic value.

The situation is more complex in the main section, where a Graetz-type problem at the polymer wall is coupled with a problem in penetration theory (Higbie, 1935) at the gas interface. Assuming such coupling to have only a minor effect, one may still use $N = 3.8$. The value of m is not constant in the axial direction, and the initial temperature distribution in the polymer phase (i.e., at the beginning of the main section) is not flat, hence penetration theory cannot in principle be used directly. However, the average value for m obtained from a penetration theory calculation is again of the order of 3.8, and we use this value as a constant one. Notice that, with this estimate, the terms $1/m$ and K/δ appearing in Eq. 20 are of comparable order of magnitude.

Now we move to consideration of the heat balance. There are four terms that need to be taken into account. There are two sources of heat, supply from the walls and frictional heating in the polymer phase, and two sinks, heating and endothermic local devolatilization rate. The last is guaranteed to be significant (since devolatilization is bound to occur), and hence all other terms can be compared to it in order to decide whether they are significant or not. When this is done, frictional heating is seen to be less than 0.1% of the heat of devolatilization. (This does not imply that the Brinkman number is negligibly small, since the comparison is based on the latent heat of devolatilization and not on the heat supply; however, the Brinkman number is in fact rather small). Thus, with λ the latent heat, c_{PP} the polymer specific heat, and c_{PG} the gas specific heat, the heat transfer equation becomes, for the symmetric flow configuration where the balance is carried out on the polymer-gas system:

$$\Phi(T_W - T) = (c_{PP}Q + c_{PG}G)\frac{dT}{dz} - \lambda\frac{dQ}{dz} \tag{21}$$

with the last term being of course zero in the heating section. The overall heat transfer coefficient Φ is given by Eq. 16. In the asymmetric case, the balance is best written only on the polymer phase.

Mass transfer

Devolatilization is a very complex phenomenon, one that involves nucleation and growth of gas bubbles, their migration to the gas interface, and their release there. Modeling such a complex phenomenon from first principles would be a formidable task. We therefore simply assume that whatever the actual mechanism of devolatilization may be, the rate of release of volatile component to the gas phase is proportional to the local driving force—that is, the difference between the local vapor pressure of the volatile $p^o(T, c)$ and the actual gas phase pressure p. With A an adjustable parameter, we thus write the mass transfer equation in the main section as follows:

$$-\frac{dQ}{dz} = A\,[p^o(T, c) - p] \tag{22}$$

The adjustable parameter A is assumed to be constant. While values of N and m in the previous subsection could be estimated *a priori* with some degree of confidence, there is no way of doing that for the parameter A, which is thus taken as a parameter adjusted to fit the data (notice that no adjustable parameter has been introduced so far). The value of A is extracted from experimental data as follows. If one begins experiments at very low flow rates, the residual mass fraction in the exit stream will be very low, and in fact very close to the equilibrium value corresponding to the flash chamber pressure. Under such conditions, the slit length is clearly overdesigned and the value of A cannot be extracted from the data. However, as the flow rate is increased, one reaches a point where the exit stream residual mass fraction significantly exceeds the equilibrium value; if the flow rate is increased beyond that, large residual mass fractions are observed, that is, the volatile component leaks out. The value of A is chosen so as to fit the measured flow rate of incipient leak. When the leak flow rate is low, practically any value of A in excess of some minimum could be used to fit the data. However, the calculated flow rate at which significant leakage begins to occur is sensitive to the value of A used in the calculation, and this has been used to establish the value used in all calculations. The value of A has been taken to be the same for all experimental conditions; of course, much better fits of the data could have been obtained by allowing A to depend on operating conditions.

Experimental Details

All experiments referred to have been performed in the Bollate Research Center of Enimont Anic. The single-slit devolatilization unit consists of a vessel in which the polymer and the volatile component are mixed; a gear pump feeds the solution to the heated slit mounted on the top of the flash tank. The tank is provided with windows and a device for sampling the polymer just at the exit from the slit. An extruder is used to pump the polymer out of the flash tank, and a vacuum pump keeps the pressure in the tank at the set value. The slit has a jacket heated by circulating oil, while all other parts of the apparatus are heated electrically. The geometry of the slit is given in Figure 3.

During a run we set the feed rate of the solution, the temperature of the heating oil, and the vacuum level in the flash tank. We monitor temperature and pressure profiles along the slit, and the residual concentration of the volatile component in the exit stream. Temperatures are measured by thermocouples at the inlet and at five positions along the slit with ther-

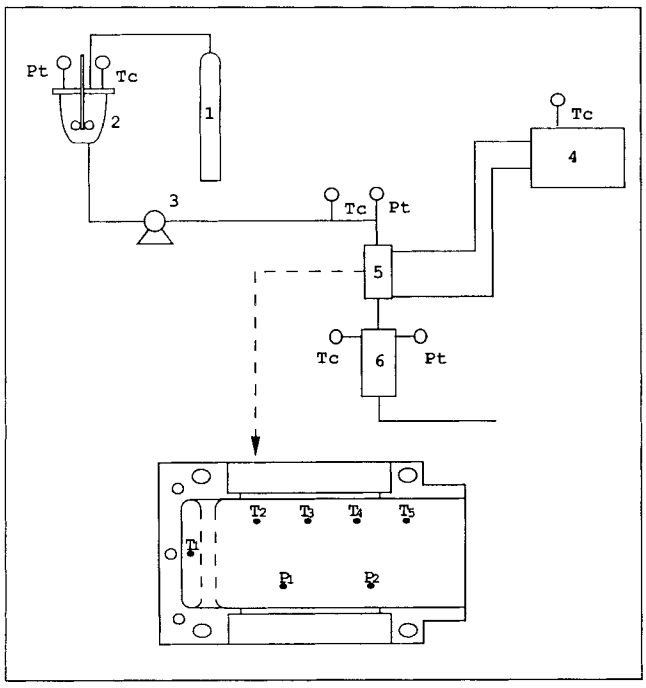

Figure 3. Geometry of single slit experimental unit.

1. Nitrogen cylinder
2. Tank
3. Pump
4. Thermostat
5. Slit
6. Vacuum chamber

mocouples of 0.25 mm dia. Pressures are measured 10 cm ahead of the inlet and at two positions along the slit: capillary tubes, filled with inert fluid, mounted flush to the wall of the slit, are connected with Druck transducers kept at a temperature lower than the temperature of the wall.

Both pressure and temperature exhibit a cyclic behavior with an excursion of the order of 0.6 bar (60 kPa) and 10°C on the average, although oscillations of up to 80°C have been observed under particular operating conditions. The feed rate is measured by a Micro Motion mass flowmeter, with an accuracy of better than 1% in the range of operation, 0 to 3 kg/h. The pressure in the flash tank is measured by a mercury vacuum gauge with readings within 1 torr (0.133 kPa).

Externally imposed conditions are held constant for at least 0.5 h before starting to record temperatures and pressures; these are then continuously monitored for 0.5 h before sampling the polymer at the exit of the slit. The analysis of the residual volatile in the polymer is performed by a conventional gas chromatographic method with a flame ionization detector. The polymer is first dissolved in $CHCl_3$, and an internal standard is added.

Nine complete sets of data have been collected and analyzed; within each set five different feed flow rates were tested, ranging from 1.39×10^{-3} to 1.39×10^{-2} kg/m·s. Wall temperatures ranged from 220° to 300°C, feed temperatures from 100° to 180°C, and flash chamber pressures from 10 to 130 mm Hg (1.33 to 17.3 kPa).

Viscosities of the polymer solutions at different temperatures and volatile concentrations have been measured in other laboratories of Montedipe. These are in reasonable agreement with the results reported by Mendelson (1976, 1980). The viscosity is proportional to the 3.4 power of molecular weight,

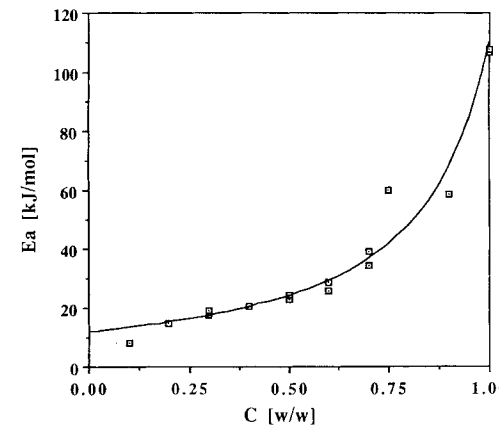

Figure 4. Activation energy for viscosity vs. polymer mass fraction.

□ experimental data (Mendelson, 1980; this study)
——— interpolation used in calculation

and, following Mendelson, to the 10.7 power of polymer weight fraction at a reference temperature of 200°C. The activation energy is strongly dependent on weight fraction, Figure 4; the interpolated curve is an inverse cubic. Data obtained at Montedipe are better correlated by using a reference temperature of 375°C, a concentration power of 4.2, and the activation energy in Figure 4. The Montedipe data are mostly at low polymer weight fractions, while the Mendelson correlation works best at high polymer weight fractions. We have used the average of the values given by the two correlations in our calculations. Unfortunately, rheological behavior is of an exponential type (large powers of both molecular weight and concentration), and discrepancies by as much as a factor of two or more between correlations and data are commonplace; pressure drops, on the other hand, are linear and not logarithmic in the viscosity.

Activity coefficients at infinite dilution have been measured by inverse chromatography, and a correlation for vapor pressure as a function of temperature and volatile mass fraction, based on these, has been developed following the methodology

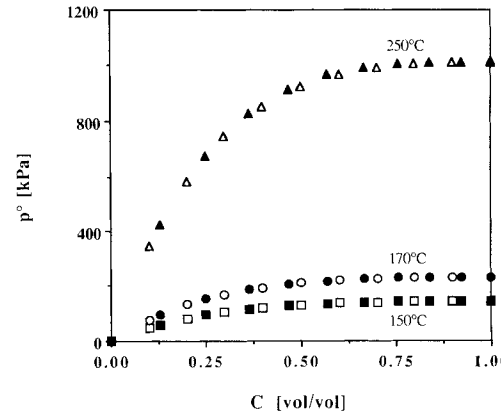

Figure 5. Vapor pressure of ethylbenzene vs. mass fraction.

▲ ■ ● model correlation
△ □ ○ Flory-Huggins eq.

presented by Holten-Anderson et al. (1986, 1987). The correlation is in very good agreement with the predictions of the Flory-Huggins equation with an interaction parameter having the value 0.4, Figure 5, and we have therefore used the latter in our calculations.

All the experiments referred to in this paper, except one set, have been performed with polystyrene, MW = 300,000 and MW/MN = 2, a Montedipe product, an ethylbenzene as the volatile component. In one set of experiments MW = 235,000 and MW/MN = 2.

Solution Procedure

Since pressure in the flash chamber, p_o, is imposed on the system, the following dimensionless variables suggest themselves naturally:

$$\text{Pressure, } \beta = \frac{p}{p_o} \tag{23}$$

$$\text{Axial position, } y = \frac{z}{L} \tag{24}$$

$$\text{Gas layer thickness, } \delta = \frac{h}{H} \tag{25}$$

$$\text{Polymer phase flow rate, } \Gamma = \frac{Q}{Q_o} \tag{26}$$

$$\text{Polymer phase viscosity, } \alpha = \frac{\mu_P}{\mu_P(T_o, c_o)} = \frac{\mu_P}{\mu_{Po}} \tag{27}$$

$$\text{Temperature, } \theta = \frac{T_w - T}{\omega} \tag{28}$$

A few comments are in order. L is the slit length, and hence $0 \le y \le 1$. δ is guaranteed to be much less than unity. β is always larger than unity, and in fact very much so over most of the slit. Γ is of order unity over the whole slit. α changes from unity at the entrance to values very much in excess of unity. θ is of course unity at the entrance, and it decreases as temperature increases (but cannot of course become negative). While $d\theta/dy$ and $d\Gamma/dy$ are at most of order unity, $d\beta/dy$ may be as large as 1,000.

In addition to the physical property ratios K and $\gamma = c_{PG}/c_{PP}$, five independent dimensionless groups arise when the equations are made dimensionless; these also contain the volatile molecular weight M and the gas constant R. The groups are:

$$B = \frac{M p_o \mu_{Po}}{4 \rho_P \mu_G R T_W} \tag{29}$$

$$D = \frac{L \mu_{Po} Q_o}{\rho_P H^3 p_o} \tag{30}$$

$$E = \frac{A p_o L}{Q_o} \tag{31}$$

$$F = \frac{3.8 L k_P \omega}{\lambda Q_o H} \tag{32}$$

$$S = \frac{c_P \omega}{\lambda} \tag{33}$$

B is the ratio of the kinematic viscosity of the polymer at the feed conditions to that of the gas at T_W and p_o; its value is of order 10. D is a dimensionless feed flow rate which also has values of order 10. E can be regarded as a modified Stanton number for the overall mass transfer coefficient A. F is a ratio of heat supply and latent heat, and is necessarily of order unity. Finally, S is a Stefan number (Stefan, 1891), the ratio of sensible and latent heats, with values of order 0.25. Should one carry over the frictional heating effect, an additional dimensionless group would arise, $p_o/\lambda\rho_P$, which has an estimated value of 10^{-6}. This group would multiply a term $d\beta/dy$ in Eq. 38 below. Since $d\beta/dy$ is at most 1,000, the frictional heating term is less than 10^{-3}. Since $d\Gamma/dy$ in Eq. 38 is guaranteed to be of order unity, neglect of frictional heating is amply justified.

Finally, a dimensionless vapor pressure function and a dimensionless viscosity function are introduced as follows, based on the fact that c is a unique function of Γ, see Eq. 15:

$$f(\theta, \Gamma) = \frac{p^o(T, c)}{p_o} \tag{34}$$

$$\alpha(\theta, \Gamma) = \frac{\mu_P(T, c)}{\mu_P(T_o, c_o)} \tag{35}$$

Equations 36–39, the governing equations of the model for the asymmetric flow configuration, in dimensionless form, are given in Table 1.

The polymer momentum balance in the main section, Eq. 36a, becomes $-d\beta/dy = 12D\alpha\Gamma$ for the symmetric flow configuration. For such a configuration the term in square brackets in Eq. 38a has a fixed value of 2. In actual fact, we have taken into account the slight variation of the latent heat with tem-

Table 1. Governing Equations of Asymmetric Flow Model

	Main Section	Heating Section	Eq. No.
Polymer momen. bal.	$-\frac{d\beta}{dy} = 3D\alpha\Gamma$	$-\frac{d\beta}{dy} = 12D\alpha$	36a,b
Mass transfer	$\frac{d\Gamma}{dy} = E(f-\beta)$	$\Gamma = 1$	37a,b
Heat transfer	$S[\Gamma + \gamma(1-\Gamma)]\frac{d\theta}{dy} + F\theta\left[1 + \frac{1}{1+3.8\,\delta/K}\right] + \frac{d\Gamma}{dy} = 0$	$S\frac{d\theta}{dy} + 2F\theta = 0$	38a,b
Gas phase moment. bal.	$1 - \Gamma = B\alpha\Gamma\delta^3\beta$	$\Gamma = 1$	39a,b

Table 2. Values of Physical Properties Used in Calculations

	Value	Source
c_{PG}	1.841×10^{3}, $m^2/s^2\cdot K$	TPM (1976)
λ	$\lambda_o[(1-T_r)/(1-T_{ro})]^{0.38}$, m^2/s^2 $\lambda_o=3.347\times10^{5}$, m^2/s^2 $T_r=T/T_C$, K $T_C=617.1$, K $T_o=409.3$, K	Watson (1943)
μ_G	8×10^{-4}, Pa·s	
k_G	1.46×10^{-2}, W/m·K	
c_{PP}	2.092×10^{3}, $m^2/s^2\cdot K$	EPSE (1985)
ρ_P	$9.5\ 10^{2}$, kg/m^3	EPSE (1985)
k_P	1.255×10^{-1}, W/m·K	EPSE (1985)

perature in our calculations, say S depends on θ for the symmetric configuration. The righthand side of Eq. 39a has to be multiplied by 4.

The heating section equations hold up to the y value where $f=\beta$; the main section equations after that. Equations 36–38 are subject to:

$$\Gamma(0)=\theta(0)=\beta(1)=1 \tag{40}$$

The boundary conditions, Eq. 40, make the problem a two-point boundary value problem. The numerical procedure we have used is as follows. Starting from a guessed value of $\beta(0)$, the heating section equations are integrated forward until $f=\beta$; from that point the main section equations are integrated forward. A simple halving convergence procedure is used to determine the new value of $\beta(0)$; this may be done even when some iteration has resulted in a negative value of $\beta(1)$, as it well may. Convergence to within a few percent of $\beta(1)=1$ is generally attained in less than twenty iterations.

A comment is needed concerning Eq. 37a. The lefthand side has an average value of 0.5: half of the feed rate becomes a gas over the slit length. β is of the order of 100 along most of the slit, and hence, should E be of order 100 or larger, the difference between f and β would be 0.1% of f. In this case, one could substitute $f=\beta$ for Eq. 37. (Mass transfer is efficient enough that, for all practical purposes, the liquid is everywhere at equilibrium with the local gas pressure.) This would collapse

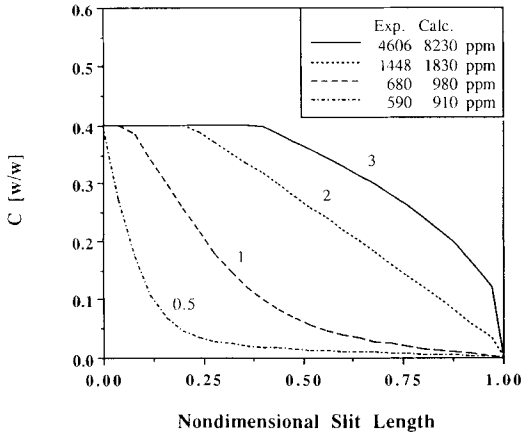

Figure 6. Calculated profiles of volatile mass fraction for four runs, $A=10^{-6}$ s/cm.

Parameter on curve is feed flow rate, kg/h
Inset: measured mass fractions in exit stream

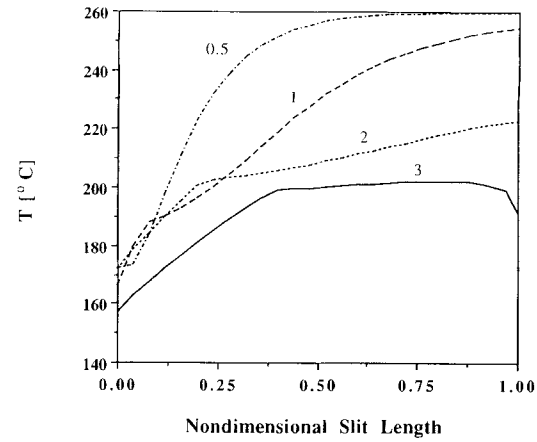

Figure 7. Calculated temperature profiles for four runs.

Parameter on curves is feed flow rate, kg/h

the problem to a single differential equation, since Eq. 36 would now yield Γ from the known value of f, and Eq. 39 would yield δ. In fact, when trying to solve numerically the full set of equations, numerical instabilities tended to occur at E values in excess of 50. This however was irrelevant, since the value of E needed to fit the data was in the numerically stable range, although in fact calculated values of f and β were indeed very close to each other.

Results

We have performed calculations corresponding to all sets of data, but here we limit ourselves to the analysis of a single set of four different flow rates. The results for all the other sets were qualitatively very similar to those discussed below. Also, we present detailed results of our calculations only for the symmetric flow configuration; except for the actual values of the pressures, the results with the asymmetric flow configuration are very similar. Values of physical properties used in our calculations are given in Table 2.

Figure 6 presents calculated profiles of volatile mass fraction. It can be seen that at the lowest flow rate devolatilization takes place early in the slit. Since the mass fraction cannot be less than that in equilibrium with the local pressure, c continues

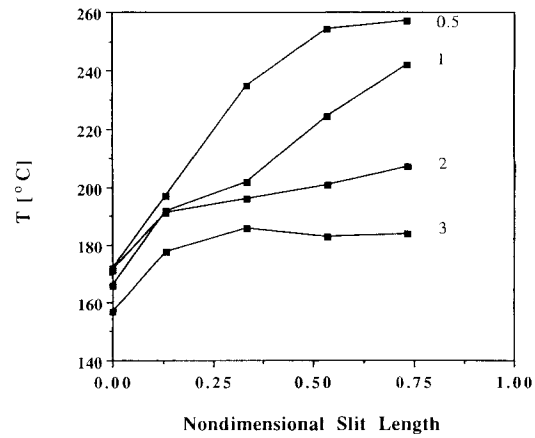

Figure 8. Measured temperature profiles for four runs.

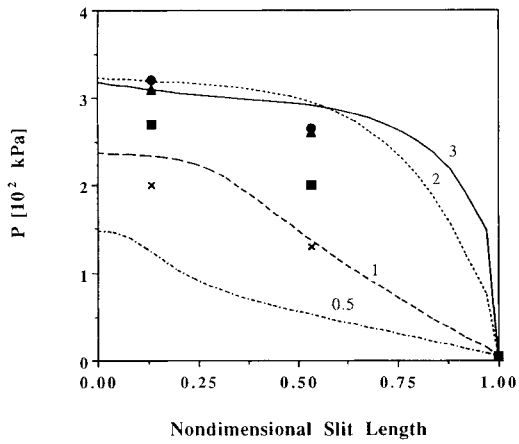

Figure 9. Calculated pressure profiles for four runs.

Measured values, kg/h: x, 0.5; ■, 1.0; ●, 2.0; ▲, 3.0

decreasing over the whole slit, simply because pressure is decreasing. At the next larger flow rate, c decreases at a more steady rate, and devolatilization is still almost complete at the exit. At the next higher flow rate the leak rate is not negligible any more, and it becomes significant at the highest flow rate. Calculated and measured values of the residual volatile at the exit are given. The uncertainty of measured values is quite large, mainly because of sampling problems; the agreement with calculated values can therefore be regarded as acceptable. In this regard, one should consider that inlet values are of the order of 500,000 ppm, so that the calculated and measured total removal rates in fact agree with each other extremely well.

Figure 7 presents calculated temperature profiles, and Figure 8 measured temperatures. At all flow rates the heating section is clearly visible as the initial region where temperature increases; as expected, its length increases with flow rate. This is followed by a rather flat region where most of the devolatilization takes place, so that the heat supplied by the wall is balanced by the latent heat. At the lowest flow rates this is followed by a final region where temperature rises again, because devolatilization is almost complete and the heat supplied by the walls is balanced by polymer heating. When the leak rate is significant, this final temperature rise does not exist, and in the extreme case there is actually a decrease—the latent heat near the exit exceeds the amount supplied by the walls. To within experimental accuracy of the data and inherent lack of precision of the model, calculated and measured values of temperature are in reasonable agreement.

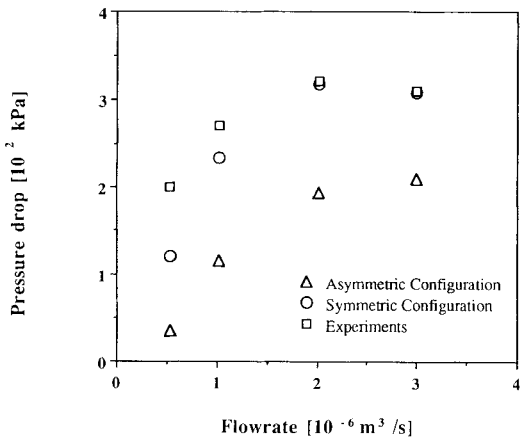

Figure 10. Calculated and measured pressure drops from first pressure gauge to exit

Figure 9 presents calculated pressure profiles, and measured values of the pressure. The latter are in practice only two points (agreement on the exit pressure value is of course intrinsic), and the comparison is only qualitative. For instance, at the lowest flow rate the pressure profile is first concave downward and then upward, and a change of curvature cannot be observed from only three points. The latter part of the profiles, where J decreases along the flow direction, is related to the temperature increase in that region, and the corresponding decrease of viscosity (little devolatilization takes place there). The other profiles are always concave downward, as the measured data also indicate. As the concentration of volatile decreases steadily, the viscosity steadily increases, in spite of any minor temperature changes.

One may notice that the calculation underpredicts the actual pressure drop at the lower flow rates. This may be due to the fact that we have used the polymer thermal conductivity, while the actual conductivity of a bubble-containing polymer is presumably lower. The effect of this approximation is worst at low flow rates, since devolatilization occurs early in the slit.

The calculated pressure profiles given in Figure 9 are for the symmetric flow configuration; the quantitative fit of the profile calculated for the asymmetric flow configuration is significantly worse. This point is borne out in Figure 10, where measured and calculated pressure drops between the first internal pressure gauge and the exit are given. It can be seen that the symmetric flow configuration gives a much better fit, and one may thus tentatively conclude that the data support the hypothesis of symmetric flow configuration. However, the uncertainty as to the appropriate values of viscosity is large enough that this cannot be construed to imply that the symmetric flow configuration is the correct one. It is also apparent that the plot of pressure drop vs. flow rate exhibits a maximum, and that all experiments have been performed near it. Indeed, the pressure drop begins decreasing with increasing flow rate when the leak rate is large, so that the average viscosity decreases as the flow rate is increased.

Conclusions

The model we have presented is in many ways a very crude one, and it could easily be improved well above its present level. First of all, it could be transformed to a full two-dimensional model: the momentum balance presented furnishes the transverse distributions of velocity at every axial position, and these could be used to solve the two-dimensional heat transfer problem exactly. This improvement would make the numerical procedure significantly more cumbersome without, presumably, resulting in a significant improvement of the predictive ability of the model.

A more important improvement would be the development of a fundamental model for the mass transfer process, leading to *a priori* estimates of the parameter A, and/or confirmation that indeed the overall rate of mass transfer is proportional to $p^o - p$. This seems a very difficult task, and it is not clear how one could attack this problem.

There is another point concerning the interaction of mass

and momentum transfer that we have left undiscussed. Devolatilization is very likely to occur via formation of gas bubbles in the polymer phase, and their subsequent growth and release to the gas phase. This implies that the polymer phase is in fact a foam rather than a pure liquid, and this casts doubt on our momentum balance in the polymer phase. This point is discussed in Appendix A. Finally, the possible formation of a shock front in the gas phase at the exit section is discussed in Appendix B.

Notation

A = mass transfer coefficient, s/m
B = ratio of reference kinematic viscosities
c = volatile weight fraction
c_o = initial value of c
c_{PP} = polymer specific heat $m^2/s^2 \cdot K$
c_{PG} = gas specific heat $m^2/s^2 \cdot K$
D = feed flow rate
E = modified Stanton number
F = ratio of heat supply and latent heat
f = vapor pressure
G = gas flow rate per unit slit width, $kg/m \cdot s$
H = slit thickness, m
h = gas layer thickness, m
J = pressure gradient, $kg/m^2 \cdot s^2$
K = ratio of conductivities
k_G = thermal conductivity of gas, $m \cdot kg/s^3 \cdot K$
k_P = thermal conductivity of polymer, $m \cdot kg/s^3 \cdot K$
M = molecular weight of volatile, kg/kmol
m = polymer Nusselt number at interface
N = polymer Nusselt number at wall
n = volume fraction of bubbles in polymer phase
p = pressure, $kg/m \cdot s^2$
p^o = vapor pressure, $kg/m \cdot s^2$
p_o = flash tank pressure, $kg/m \cdot s^2$
Q = polymer flow rate per unit width, $kg/m \cdot s$
Q_o = initial value of Q, $kg/m \cdot s$
R = gas constant, $m^2 \cdot kg/s^2 \cdot kmol \cdot K$
r = bubble radius, m
S = Stefan number
T = temperature, K
T_I = interface temperature, K
T_W = wall temperature, K
T_o = feed temperature, K
U = velocity at interface, m/s
v = local velocity, m/s
x = distance from gas wall, m
y = axial position
z = axial position, m

Greek letters

α = viscosity ratio
β = pressure
γ = specific heat ratio
Γ = polymer flow rate
δ = gas layer thickness
ϵ = viscosity ratio
θ = temperature
λ = latent heat of devolatilization, $kg \cdot m^2/kmol \cdot s^2$
μ = viscosity of fluid surrounding droplets, $kg/m \cdot s$
μ' = viscosity of droplets fluid, $kg/m \cdot s$
μ_P = polymer viscosity, $kg/m \cdot s$
μ_{Po} = feed viscosity, $kg/m \cdot s$
μ_G = gas viscosity, $kg/m \cdot s$
ρ_G = gas density, kg/m^3
ρ_P = polymer density, kg/m^3
σ = surface tension, kg/s^2
τ = shear stress, $kg/m \cdot s^2$
τ_o = shear stress at gas wall, $kg/m \cdot s^2$
Φ = heat transfer coefficient, $kg/s^3 \cdot K$
χ = shear rate, s^{-1}
ω = temperature driving force, K

Literature Cited

Batchelor, G. K., *An Introduction to Fluid Dynamics,* Cambridge Univ. Press (1967).
Bird, R. B., W. R. Stewart, and E. N. Lightfoot, *Transport Phenomena,* Wiley, New York (1960).
Charles, M. E., and L. U. Lillehet, "Cocurrent Stratified Laminar Flow of Two Immiscible Liquids in a Rectangular Duct," *Can. J. Chem. Engr.,* **43**(6), 110 (1965).
Charles, M. E., and P. J. Redberger, "The Reduction of Pressure Gradients on Oil Pipelines by the Addition of Water, Numerical Analysis of Stratified Flow," *Can. J. Chem. Eng.,* **40**(4), 70 (1962).
Drew, T. B., "Mathematical Attacks on Forced Convection Problems: A Review," *Trans. AIChE,* **26**, 26 (1931).
Dukler, A. E., M. Wicks III, and R. G. Cleveland, "Frictional Pressure Drop in Two-Phase Flow. B: An Approach through Similarity Analysis," *AIChE J.,* **10**, 44 (1964).
Einstein, A., "Eine Neue Bestimmung der Molekul-Dimensionen," *Ann. Physik,* **19**, 289 (1906).
Einstein, A., "Berichtigung zu Meiner Arbeit: Eine Neue Bestimmung der Molekul-Dimensionen," *Ann. Physik,* **34**, 591 (1911).
EP, European Patent 352727 (1990).
EPSE, *Encyclopaedia of Polymer Science and Engineering,* 2d ed., Wiley Interscience, New York (1985).
Higbie, R., "The Rate of Absorption of a Pure Gas into a Still Liquid During Short Times of Exposure," *Trans. AIChE,* **31**, 365 (1935).
Hinata, S., and M. Ohki, "Relation Between Apparent Viscosity and Void Fraction in Two-Phase Flow," *Bull. JSME,* **75**, 951 (1971).
Holten-Andersen, J., A. Fredenslund, R. Rasmussen, and G. Carvoli, "Phase Equilibria in Polymer Solutions by Group Contribution," *Fluid Phase Eq.,* **29**, 357 (1986).
Holten-Andersen, J., P. Rasmussen, and A. Fredenslund, "Phase Equilibria of Polymer Solutions by Group Contribution. 1: Vapor-Liquid Equilibria," *Ind. Eng. Chem. Res.,* **26**, 1382 (1987).
Jacob, M., *Heat Transfer,* Wiley, New York (1949).
Maffettone, P. L., and G. Astarita, "Modeling of Slit Devolatilization of Polymers," Paper 5E1, Eur. Meet. Rheology—Brit. Soc. Rheol. Meet., Edinburgh, September 1990.
Medvedev, V. F., "Viscosity of Gas-Containing Liquids," *Zh. Prikl. Kim.,* **55**, 451 (1982).
Mendelson, R. A., "A Generalized Melt Viscosity-Temperature Dependence for Styrene-Acrylonitrile Based Polymers," *Pol. Eng. Sci.,* **16**, 690 (1976).
Mendelson, R. A., "Concentrated Solution Viscosity Behavior at Elevated Temperatures. Polystyrene in Ethylbenzene," *J. Rheol.,* **24**, 765 (1980).
Navratil DiAndreth, A., "Two-Phase Flow in Screw Extruders," PhD Thesis, Univ. Delaware (1984).
Pal, R., and E. Rhodes, "Viscosity/Concentration Relationships for Emulsions," *J. Rheol.,* **33**, 1021 (1989).
Stefan, J., "Ueber die Theorie der Eisbildung insbesonderen ueber die Eisbildung in Polarmeere," *Ann. Phys. Chem.,* NF**42**, 261 (1891).
Taylor, G. I., "The Viscosity of a Fluid Containing Small Drops of Another Fluid," *Proc. Roy. Soc., A.,* **138**, 41 (1932).
TPM, *Thermophysical Properties of Matter,* **6**, suppl., Plenum, New York (1976).
Watson, K. M., "Thermodynamics of the Liquid State. Generalized Predictions of Properties," *Ind. Eng. Chem.,* **35**, 398 (1943).
Yu, H. S., and E. M. Sparrow, "Stratified Laminar Flow in Ducts of Arbitrary Shape," *AIChE J.,* **13**, 10 (1967).

Appendix A: Effect of Gas Bubbles in Liquid Phase

The equivalent viscosity μ^* of a suspension of spherical droplets of liquid of viscosity μ' into a liquid of viscosity μ was analyzed by Taylor (1932). With n the volume fraction of suspended droplets, the result is:

$$\mu^* = \mu\left(1 + 2.5n\frac{\mu' + 0.4\mu}{\mu' + \mu}\right) \tag{A1}$$

When the viscosity of the droplets is very high, this reduces

to the Einstein (1906, 1911) result for a suspension of solid spheres, $\mu^* = \mu(1 + 2.5n)$. For the converse case, which is of interest here, where the viscosity of the droplets phase is negligible, one obtains $\mu^* = \mu(1 + n)$. It is perhaps slightly surprising that the presence of gas bubbles (endowed with zero viscosity) should increase the equivalent viscosity of the suspension, but that is in fact the result. Experimental verification of this result is provided by Hinata and Ohki (1971). Medvedev (1982) suggests that $\mu^* = \mu/(1 - n)$ is a better correlation of the Hinata and Okhi data, which do extend into values of n large enough that the Taylor result does not hold. To within order n, which is the theoretical limit of the Taylor result, the two equations coincide.

Taylor also provides an estimate of the largest bubble radius for which the bubbles will in fact remain spherical. This is obtained as follows. It is impossible to impose the condition that velocity, as well as all three components of stress, be continuous across the interface, and hence one concludes that the normal stress is in fact discontinuous. One then requires this discontinuity—which by itself would tend to distort the bubbles—to be less than the surface tension σ divided by the bubble radius r. With χ the shear rate imposed in the suspension, the condition for sphericity is:

$$r < \frac{\sigma}{(2\mu\chi)} \tag{A2}$$

There are numerous difficulties if one tries to apply these results to the problem at hand. First, we do not have a reliable estimate of the bubble volume fraction n, and in fact it seems likely that n changes along the flow direction. Second, the condition of Eq. A2 is hard to satisfy in high-viscosity liquids such as are of interest in our case. $\mu\chi$ is of course the shear stress in the polymer, and its order of magnitude is obtained from the measured pressure drops; it is typically 4,000 $kg/m \cdot s^2$. The surface tension is not known, but even assuming it to be as large as that of water, 0.07 kg/s^2, Eq. A2 would be satisfied only by ridiculously small bubbles. One thus concludes that the bubbles do get severely distorted, and there is no theoretical analysis for the latter case.

There are numerous empirical correlations for the equivalent viscosity of emulsions, and these are critically reviewed by Pal and Rhodes (1989); approaches based on the concept of an equivalent homogeneous phase are reviewed by Dukler et al. (1964). For at least some of the proposed correlations, as a crude first-order approximation, the viscosity is actually smaller than that of the surrounding liquid, say $\mu^* = \mu(1 - n)$. However, the volumetric flow rate of the emulsion phase would be $1/(1 - n)$ times that which would prevail in the absence of bubbles. Since the pressure gradient is proportional to the product of viscosity and volumetric flow rate, at this level of approximation the effect of gas bubbles cancels out.

Appendix B: Speed of Sound in Gas Layer

At the exit of the slit, the gas volumetric flow rate is very high, and one needs to address the question of a possible shock front in the gas. The analysis to be developed depends weakly on temperature (only the square root of its absolute value enters the equations), and we here consider an exit temperature of 550 K, for which the speed of sound is 265 m/s. The velocity of the gas phase at the exit of the slit calculated from our equations increases with increasing Q_o as long as devolatilization is almost complete; hence the highest gas flow rate is attained at Q_o values of the order of 10^{-2} kg/m·s. With $c_o = 0.5$, and assuming complete devolatilization, at an exit pressure of 4×10^3 $kg/m \cdot s^2$ (0.04 atm) one would calculate a velocity of 325 m/s, which is supersonic. The ratio $325/265 = 1.23$ is, however, not very large: under these extreme conditions, one would estimate an actual pressure at the exit section of 0.049 atm (with a shock right at the exit). Since 0.049 atm is still very significantly less than the pressure over most of the slit, the calculation based on our model is still essentially correct. Again, it would be easy to include a correction for this effect by requiring the exit pressure to be the largest one between that actually imposed in the flash chamber and the one corresponding to the gas moving at the speed of sound at the exit section.

Manuscript received Dec. 18, 1990, and revision received Mar. 15, 1991.